Color restoration method for underwater objects based on multispectral images

Yilu Guo[1,2], Hongbo Liu[1], Yao Chen[1], Waqar Riaz[3], Ping Yang[4], Hong Song[1,*], Ye Shen[1], Shuyue Zhan[1], Hui Huang[1], Hangzhou Wang[1], Meifen Fang[5], Jianxing Leng[1]
1. Ocean College, Zhejiang University, Zhoushan, 316021,China
2. State Key Laboratory of Satellite Ocean Environment Dynamics (Second Institute of Oceanography, SOA), Hangzhou, 310012, China
3. Hamdard Institute of Engineering and Technology, Hamdard University, Karachi, Pakistan
4. School of Digital Media, Hangzhou Dianzi University, Hangzhou, 310018, China
5. Blue-Science Opto-Electronics Co. Ltd., Hangzhou, 310018, China
*Corresponding author: hongsong@zju.edu.cn

***Abstract*—Perceiving color in water medium is always challenging due to the dense non-uniform attenuation and scattering of light across the visible spectrum. This paper presents a color restoration method for underwater objects based on multispectral images. To begin with, underwater multispectral images are obtained and restored with the influence of attenuation and scattering being eliminated by an in-suit restoration algorithm, and later on color images are restored from the multispectral images. Assessment of the restored color images and images taken by color camera in air medium authenticates the accuracy of the restoration method.**

Key words—underwater multispectral imaging, underwater color restoration

I. Introduction

Observing color in underwater environment is important because it is attentively concerned to the health condition of innumerable living species, such as coral, shells, and some kinds of sea grasses. Moreover, color images have less redundant information than multispectral images that are easier to observe. However, capturing underwater color is challenging due to the strong uneven attenuation and scattering of light in water across the visible spectrum, which respectively shifts the dramatic hue toward green and hazes the underwater images.

Recent work in color restoration has shown impressive results for both compensating attenuation and reducing scattering. For example, Ahlen [1] uses a spectrometer to measure the reflected spectrum of a referenced gray target in different underwater depths, estimates the attenuation coefficients of water, and reimburses the images according to Beer-Lambda law. In procession, the method is further developed on different aspects, such as acquirement of attenuation coefficients directly by camera, consideration of strobe's light pattern, etc. [2-4]. Yang [5] eliminates the haze using Dark-channel prior method, and then restores color balance using Unsupervised Color Correction Method, which is based on the contrast correction of RGB and HSI color model [6].

In this paper, color restoration method is proposed for underwater objects based on multispectral images. Both the impact of attenuation and scattering on images are calibrated from images of same object on various depth, and then eliminated by a multispectral image restoration method. With an algorithm based on our model, color images are restored from multispectral images. And comparison between restored color images and images taken by color camera in the medium of air is made to validate the accuracy of the restoration method.

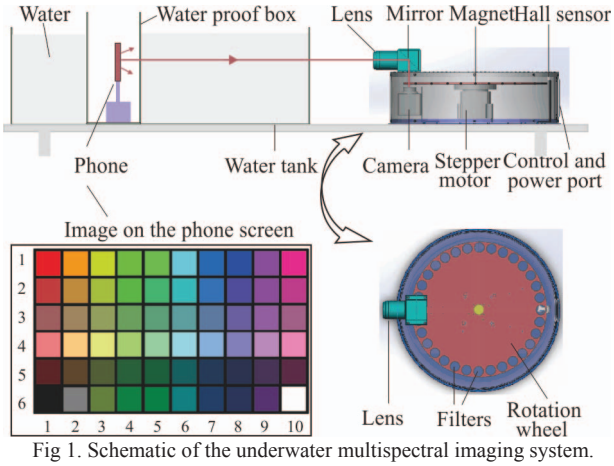

Fig 1. Schematic of the underwater multispectral imaging system.

II. Experiment Setup & Methods

A. Underwater multispectral imaging system

A system representing the underwater multispectral imaging setup in Fig. 1, chiefly resides a mobile phone, a water tank and established multispectral imaging system. The mobile phone (Xiaomi 3, Xiaomi, China) with an LCD screen (IPS, Sharp, Japan) is used as underwater object to be imaged displaying 60 different color pieces on a full screen. The color pieces are basically squares in aligned as 6 rows and 10 columns. Each column presents a hue of the Munsell color system, and each row presents different combinations of value and Chroma.

The water proof box (L35×W25×H50 cm) is made of 6 mm-thick quartz glass, and the water tank (L300×W30×H30 cm), made of 10 mm-thick transparent quartz glass, is occupied with clean pipe water.

The multispectral imaging system is placed out of the water tank. It primarily involves an imaging lens, a mirror, a rotation

978-1-4673-9724-7/16/$31.00 ©2016 IEEE

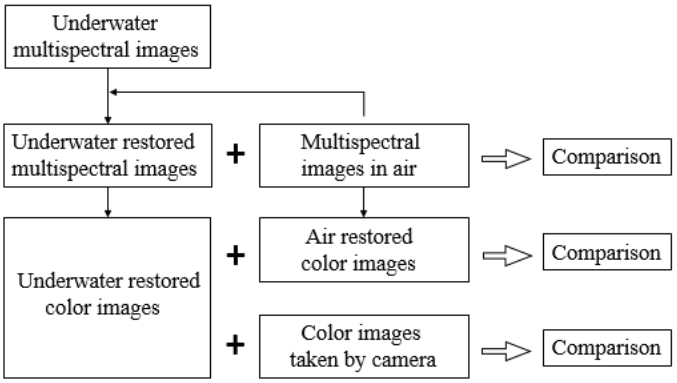

Fig. 2. Flow chart of color restoration based on multispectral images.

filter wheel with a set of filters and a monochrome CCD camera. The lens is a cemented doublet (GCL-010607, Daheng, China), with a focal length of 150 mm and a diameter of 38.1 mm. Computing device is used to operate Rotation filter wheel which installed with 15 filters whereas each coupled with a tiny magnet alongside. The wheel is driven by a stepper motor with the rotation angle monitored by a Hall sensor. The filters (FB serious, Thorlabs, USA) on the wheel have a FWHM of 10 nm, with the center wavelength ranging from 420 nm to 700 nm at an interval of 20 nm. The camera (Lm-165M, Lumenera, USA) has a resolution of 1392×1040 pixels and a dynamic range of 66 dB. During image acquisition, the filters are successively spun onto the light axis of camera, and remains on the axis until the camera is entirely exposed.

B. Image collection & processing

Initially, color images of the phone are assembled at an imaging distance of 340 cm in a dark environment by a color camera (MER-030-120UC-L, Daheng, China) with an image lens (M5018MP, Computar, Japan), which are used as references for restored color images. Then multispectral images in medium of air are collected, with the color camera replaced by the multispectral imaging system discussed above. Finally, underwater multispectral images are captured in water medium at diverse distances of 10 cm, 20 cm till 260 cm.

Later the investigation just debated earlier, multispectral images are processed to create color images. This work mainly includes underwater multispectral image restoration and color restoration from multispectral images. Fig 2 shows the flow chart of the experiment attempted. Further discussion for the work has been debated in the following subsections.

C. Underwater multispectral image restoration

The schematics for multispectral imaging in air and underwater in paraxial condition are illustrated in Fig. 3(a) and Fig. 3(b), respectively. It can be observed that underwater images are differ from air images in two aspects:

(1) Intensity changes due to attenuation and scattering caused by water, and reflection by glass,

(2) Refraction due to the change of refractive index in the direction of light path.

According to geometrical optics theory and Jaffe-McGlamery approach [7 - 8], relationship between brightness of image in air and water medium can be deduced as

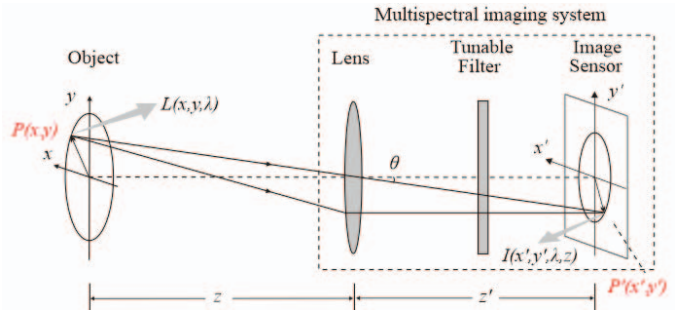

(a) Air Multispectral imaging in air medium

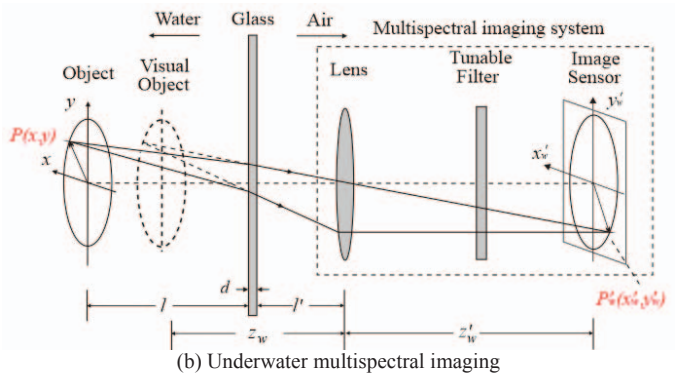

(b) Underwater multispectral imaging

Fig.3.Illustration of multispectral imaging in the medium of air and underwater

$$I_w(i_w, j_w, \lambda_c, z_w) = \frac{G(z_w)}{G(z)} \underbrace{\beta(\lambda_c) e^{-\alpha(\lambda_c) l}}_{k(\lambda_c, l)} I(i, j, \lambda_c, z) + \underbrace{\kappa(\lambda_c) e^{-\upsilon(\lambda_c)} + \gamma(\lambda_c)}_{b(\lambda_c, l)} \quad (1)$$

where

$$G(z_w) = \left(\frac{z_w - f}{z_w}\right)^2, G(z) = \left(\frac{z - f}{z}\right)^2 \quad (2)$$

In which $I_w(i_w, j_w, \lambda_c, z_w)$ and $I(i, j, \lambda_c, z)$ is the brightness of a coordinate point (i_w, j_w) and (i, j) in water and air respectively, with a center wavelength of λ_c, the element $G(z_w)$ and $G(z)$ shows how refraction affects the irradiance, $\beta(\lambda_c)$ is the effect of refraction, $\alpha(\lambda_c)$ is the attenuation coefficient affected by water, $\kappa(\lambda_c) e^{-\upsilon(\lambda_c)}$ represents the influence of hazing cause by scattering, $\gamma(\lambda_c)$ represents stray light, and f is the focus length of lens. z_w, z and l is distances shown in Fig.3.

Define a coefficient vector as $\Phi(\lambda) = [a(\lambda), \nu(\lambda), \beta(\lambda), \kappa(\lambda), \gamma(\lambda)] \in R^5$. If all coefficients in $\Phi(\lambda)$ are known, the energy losses in underwater images can be rectified based on the relationship in (1). In what follows a brief introduction of my way to calibrate the coefficients ***in-suit*** are given.

For the 60 different color pieces on the phone screen, a set of equations can be constructed as

$$\begin{cases} I_w(i_{w,1}, j_{w,1}, \lambda_1, z_{w,1}) = \frac{G(z_{w,1})}{G(z)} k(\lambda_1, l_1) I(i_1, j_1, \lambda_1, z) + b(\lambda_1, l_1) \\ I_w(i_{w,1}, j_{w,2}, \lambda_1, z_{w,1}) = \frac{G(z_{w,1})}{G(z)} k(\lambda_1, l_1) I(i_1, j_2, \lambda_1, z) + b(\lambda_1, l_1) \\ \vdots \\ I_w(i_{w,10}, j_{w,6}, \lambda_1, z_{w,1}) = \frac{G(z_{w,1})}{G(z)} k(\lambda_1, l_1) I(i_{10}, j_6, \lambda_1, z) + b(\lambda_1, l_1) \end{cases} \quad (3)$$

Writing (3) in matrix form, we have a matrix equation as

$$\underbrace{\begin{bmatrix} \frac{G(z_{w,1})}{G(z)} I(i_1, j_1, \lambda_1, z) \\ \frac{G(z_{w,1})}{G(z)} I(i_1, j_2, \lambda_1, z) \\ \vdots \\ \frac{G(z_{w,1})}{G(z)} I(i_{10}, j_6, \lambda_1, z) \end{bmatrix}}_{D} \underbrace{\begin{bmatrix} k(\lambda_1, l_1) \\ b(\lambda_1, l_1) \end{bmatrix}}_{X} = \underbrace{\begin{bmatrix} I_w(i_{w,1}, j_{w,1}, \lambda_1, z_{w,1}) \\ I_w(i_{w,1}, j_{w,2}, \lambda_1, z_{w,1}) \\ \vdots \\ I_w(i_{w,10}, j_{w,6}, \lambda_1, z_{w,1}) \end{bmatrix}}_{Y} \quad (4)$$

The unknown terms $k(\lambda_c, l)$ and $b(\lambda_c, l)$ can be estimated by solving (3) with linear least square (LLS) method as

$$\hat{X} = (D^T D)^{-1} D^T Y \quad (5)$$

where $\hat{X}$ determines the value of unknown X.

To have an assessed of water attenuation coefficient $\alpha(\lambda_c)$, underwater images that was captured at different distances can be used. According to the definition of $k(\lambda_c, l)$ in (1), a set of equations can be developed for a series of underwater distances as

$$\beta(\lambda_1) \underbrace{\begin{bmatrix} e^{-\alpha(\lambda_1) l_1} \\ e^{-\alpha(\lambda_1) l_2} \\ \vdots \\ e^{-\alpha(\lambda_1) l_M} \end{bmatrix}}_{P(\alpha)} = \underbrace{\begin{bmatrix} k(\lambda_1, l_1) \\ k(\lambda_1, l_2) \\ \vdots \\ k(\lambda_1, l_M) \end{bmatrix}}_{K} \quad (6)$$

Unknowns $\alpha(\lambda_c)$ and $\beta(\lambda_c)$ can be estimated by solving an optimization problem as

$$\hat{\alpha}(\lambda_1), \hat{\beta}(\lambda_1) = \arg \min_{\alpha^*, \beta^*} \underbrace{\|K - \beta^* P(\alpha^*)\|_2^2}_{J} \quad (7)$$

where J is the cost function to be minimized by the optimization algorithm. $\hat{\alpha}(\lambda_1)$ and $\hat{\beta}(\lambda_1)$ are the estimates of $\hat{\alpha}(\lambda_1)$ and $\hat{\beta}(\lambda_1)$, respectively.

Similarly, another set of equations to mathematically visualize the hazing coefficients is formed as

$$\kappa(\lambda_1) \underbrace{\begin{bmatrix} e^{-\nu(\lambda_1) l_1} \\ e^{-\nu(\lambda_1) l_2} \\ \vdots \\ e^{-\nu(\lambda_1) l_M} \end{bmatrix}}_{Q(\nu)} + \gamma(\lambda_1) = \underbrace{\begin{bmatrix} b(\lambda_1, l_1) \\ b(\lambda_1, l_2) \\ \vdots \\ b(\lambda_1, l_M) \end{bmatrix}}_{B} \quad (8)$$

Coefficients $\nu(\lambda_1)$, $\kappa(\lambda_1)$and $\gamma(\lambda_1)$ are valued by solving an optimization problem as

$$\hat{\nu}(\lambda_1), \hat{\kappa}(\lambda_1), \hat{\gamma}(\lambda_1) = \arg \min_{\nu^*, \kappa^*, \gamma^*} \underbrace{\|B - \gamma^* - \kappa^* Q(\nu^*)\|_2^2}_{J'} \quad (9)$$

where J' is the cost function to be lessened by the optimization algorithm. $\hat{\nu}(\lambda_1)$, $\hat{\kappa}(\lambda_1)$ and $\hat{\gamma}(\lambda_1)$ are the evaluates of $\nu(\lambda_1)$, $\kappa(\lambda_1)$ and $\gamma(\lambda_1)$ respectively.

By repeating the procedures above for different wavelengths $\lambda_c = \lambda_1, \lambda_1, \cdots, \lambda_p$ (where p is the number of wavelengths to be tuned in the multispectral imaging system), the coefficients in Φ(λ) can be estimated.

With coefficients estimated earlier, following (1), the underwater images can be restored as

$$\hat{I}_w(i_w, j_w, \lambda_c, z_w) = \frac{G(z)}{G(z_w)} [\hat{\beta}^{-1}(\lambda_c) e^{\hat{\alpha}(\lambda_c) l} (I_w(i_w, j_w, \lambda_c, z_w) - \hat{\kappa}(\lambda_c) e^{-\hat{\nu}(\lambda_c)} - \hat{\gamma}(\lambda_1))] \quad (10)$$

where $\hat{I}_w(i_w, j_w, \lambda_c, z_w)$ are the image brightness after restoration.

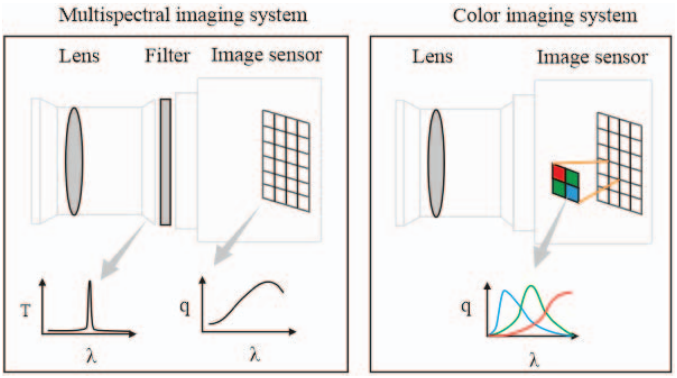

Fig.4 Illustration of multispectral imaging system and color imaging system

The accuracy of restoration is calculated by Residual and Relative residual, which are defined as

$$Residual = \left|\hat{I}_w(i_w, j_w, \lambda_c, z_w) - I(i_1, j_1, \lambda_1, z)\right| \quad (11)$$

$$Relative\ residual = \frac{|\hat{I}_w(i_w, j_w, \lambda_c, z_w) - I(i_1, j_1, \lambda_1, z)|}{I(i_1, j_1, \lambda_1, z)} \quad (12)$$

In this work we use the image cubes captured water medium at distances of 60 cm-160 cm for coefficients calibrations and the rest for checking of results.

D. Real color image restoration

As shown in Fig.4, the multispectral imaging system is differ from color imaging system on the phenomenon of splitting of light. Assuming a point on the targeted object has spectrum denoted as $I(x, y, \lambda)$, the response of color imaging system can be expressed as [9]

$$I_f(x, y) = k_1 \int I(x, y, \lambda) q_f(\lambda)\, d\lambda$$
$$= k_1 \sum_\lambda I(x, y, \lambda) q_f(\lambda), f \in (r, g, b) \quad (13)$$

where $f \in (r, g, b)$ represent the *r,g,b* channel of camera, $I_f(x, y)$ is the response of the camera on pixel (x,y), and $q_f(\lambda)$ is the quantum efficiency (or spectral response) of the camera. k_1 is a factor that changes with exposure time, lens diameter, etc. To get a standard expression of color that free from proprieties of lens or exposure time, the response of color is stabilized by

$$I_{Nf}(x, y) = \frac{I_f(x,y)}{Max\{I_f(x,y)\}} \quad (14)$$

where $Max\{I_f(x, y)\}$ is the maximum response among all pixels and all channels.

While the response of multispectral imaging system can be expressed as

$$I_m(x, y, \lambda) = k_2 \int I(x, y\lambda) T(\lambda) q(\lambda)\, d\lambda \quad (15)$$

where $T(\lambda)$ is the transmittivity function of filter, and $q(\lambda)$ is the spectral response (or quantum efficiency) of the camera. The filter used in the multispectral system has narrow pass band, thus $T(\lambda)$ can be seen as an impulse function at its center wavelength λ_c and (13) can be developed as

$$I_m(x, y, \lambda_c) = k_2\, I(x, y, \lambda_c) q(\lambda_c) T(\lambda_c) \quad (16)$$

With different filters, multispectral images are obtained with the spectrum of the object being sampled. For the reason $q(\lambda_c)$

and $T(\lambda_c)$ vary with wavelength, the obtained spectrum is distorted by them.

To restore color from multispectral images, primarily, the distortion of object spectrum generated by filter and camera is corrected by the given equation

$$I_s(x,y,\lambda_c) = \frac{I_m(x,y,\lambda_c)}{q(\lambda_c)T(\lambda_c)} \tag{17}$$

where $I_s(x,y,\lambda_c)$ is the corrected spectral intensity, occurred as a sampling results of object spectrum. Then the corrected spectrum is linear interpolated with the algorithm will be

$$\frac{I_L(x,y,\lambda_{c0})-I_S(x,y,\lambda_{c1})}{\lambda_{c0}-\lambda_{c1}} = \frac{I_S(x,y,\lambda_{c2})-I_S(x,y,\lambda_{c1})}{\lambda_{c2}-\lambda_{c1}} \tag{18}$$

where $\lambda_{c0}\epsilon[\lambda_{c1},\lambda_{c2}]$ is the wavelength for interpolation, λ_{c1} and λ_{c2} are adjacent wavelengths of multispectral system, and $I_L(\lambda_{c0})$ is the interpolated spectral intensity of λ_{c0}. In this work the interpolated spectrum has a resolution of 5 nm. Then color restoration is achieved by simulating the image processing in (13), namely, calculating the color response by

$$\begin{aligned}\tilde{I}_f(x,y) &= k_3 \int I_L(x,y,\lambda) q_f(\lambda)\, d\lambda \\ &= k_3 \textstyle\sum_{\lambda_{c0}} I_L(x,y,\lambda_{c0}) q_f(\lambda_{c0}),\ f \in (r,g,b)\end{aligned} \tag{19}$$

where $\tilde{I}_f(x,y)$ is the restored color of f channel, and k_3 is a normalization coefficient that is calculated by

$$k_3 = \frac{1}{\max\{\sum_{\lambda_{c0}} I_L(x,y,\lambda_{c0}) q_f(\lambda_{c0})\}} \tag{20}$$

III. Results

A. Underwater multispectral image restoration

In Fig.5, the raw underwater images, the images after the implementation of restoration and the images in air medium are shown for comparison of their intensity. It can be seen that underwater images are seriously darken by water, while the restored images have almost the same brightness with images in air medium.

Fig.7 shows how image intensity changes with wavelength and underwater distance. In Fig.7 (a) spectrums of color piece (4,4) and mean spectrum of all color piece are shown. It can be understood that the restored curves of the six different underwater distances and the air curves almost overlapped with the residual value of less than 0.02. In Fig.7 (b) the relationships between the intensity of 440 nm, 520 nm, 560 nm, and 600 nm on piece (4,4) and distances are shown, in which the restoration relative residual are less than 10%. The mean residual for all pieces is 0.0022 and the mean relative restoration error is 5.25%, indicating accurate restoration of the spectral energy.

B. Real color image restoration

In Fig.6 restored color images obtained from multispectral images are shown. It can be seen that the color of underwater images is faint, while the images created from the restored multispectral images are colorful and vibrant. The color of Fig.6 (b), (c), and (d) are quite similar, showing good restoration results.

IV. Conclusion

In this paper we have proposed an underwater color restoration method based on multispectral images. Firstly, an underwater multispectral image restoration method is proposed to eliminate the disturbance by water, with the restoration residual and relative residual being calculated as 0.02 and 5.25% on average, respectively. Real color images are restored from the underwater multispectral images by a real color restoration algorithm. As a result, the restoration images have similar color with images taken in medium of air by color camera, thus the proposed restoration method are proved.

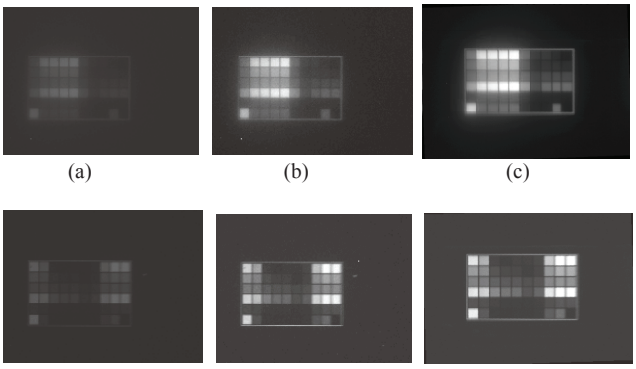

Fig.5 Multispectral images. (a) Underwater multispectral image of 460 nm in water medium with underwater distances of 240 cm. (b) Restored image of (a). (c) Image in air medium of 460 nm. (d) Underwater multispectral image of 620 nm with underwater distances of 240 cm. (e) Restored image of (d). (f) Air medium image of 620 nm.

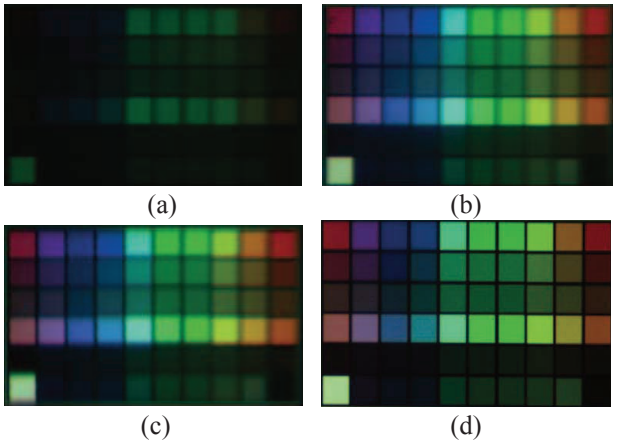

Fig.6 Color images of the phone, among which (a) is created from raw underwater multispectral images in medium of water with underwater distance of 240 cm, (b) is created from restored multispectral images, (c) is created from multispectral images in air medium, and (d) is imaged by color camera in air medium.

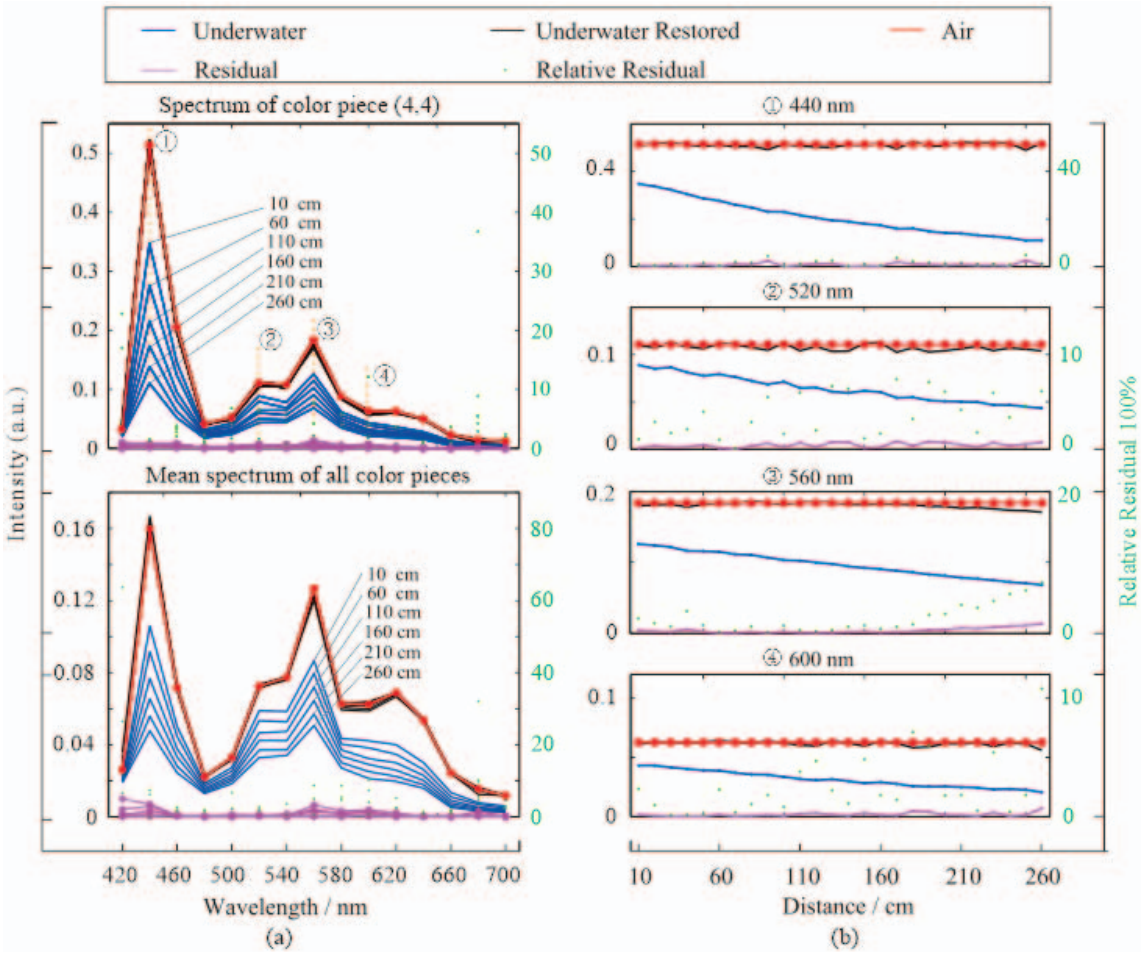

Fig.7 The relationship of wavelength and image intensity. (a) Spectrum of color piece (4,4) and mean spectrum of all the 60 color pieces. (b) Relationship between underwater distance and image intensity of 440 nm, 520 nm, 560 nm and 600 nm on color piece (4,4).

ACKNOWLEDGMENT

The work is financially supported by the National High-tech R&D Program of China (863 Program) (No. 2014AA093400), National Natural Science Foundation of China (NO. 11304278) and Open Fund of State Key Laboratory of Satellite Ocean Environment Dynamics (No. SOED1606).

REFERENCE

[1] J. Ahlen, E. Bengtsson, and D. Sundgren, "Evaluation of underwater spectral data for colour correction applications," Proceedings of the 5th WSEAS International Conference on Circuits, Systems, Electronics, Control & Signal Processing (World Scientific and Engineering Academy and Society, 2006), 2005, pp. 321–326

[2] A. Yamashita, M. Fujii, and T. Kaneko, "Color registration of underwater images for underwater sensing with consideration of light attenuation," Robotics and automation, 2007 IEEE international conference on, 2007, pp. 4570–4575.

[3] J. Kaeli, H. Singh, C. Murphy, and C. Kunz, "Improving color correction for underwater image surveys," Proceedings of IEEE/MTS OCEANS'11, 2011, pp. 805–810.

[4] Bongiorno, D. L., Bryson, M., & Williams, S. B. (2013, June). Dynamic spectral-based underwater colour correction. Proceedings of IEEE/MTS, OCEANS'13, 2013, pp. 1-9.

[5] H. Y. Yang, P. Y. Chen, C. C. Huang, Y. Z. Zhuang, and Y. H. Shiau, "Low complexity underwater image enhancement based on dark channel prior," Proceedings of International Conference on Innovations in Bioinspired Computing and Applications, 2011, pp. 17–20.

[6] K. Iqbal, M. Odetayo, A. James, R. A. Salam, "Enhancing the low quality images using Unsupervised Colour Correction Method". Systems Man and Cybernetics (SMC), 2010 IEEE international conference on, 2010. pp. 1703-1709.

[7] X. Li and Z. Ceng, Geometrical optics, aberrations and optical design, 2nd ed. Zhejiang University, 2007.

[8] J. S. Jaffe, "Computer modeling and the design of optimal underwater imaging systems," Oceanic Engineering, IEEE Journal of 15, 1990, pp. 101–111.

[9] S. Lin and L. Zhang, "Determining the radiometric response function from a single grayscale image," Proceedings of IEEE Computer Society Conference on Computer Vision and Pattern Recognition, 2005, pp. 66–73.